Thermodynamic assessment of the aluminum corner of the Al-Fe-Mn-Si system

Jacques Lacaze, Luiz Eleno, Bo Sundman

Thermodynamic Assessment of the Aluminum Corner of the Al-Fe-Mn-Si System

JACQUES LACAZE, LUIZ ELENO, and BO SUNDMAN

A new assessment of the aluminum corner of the quaternary Al-Fe-Mn-Si system has been made that extends beyond the COST-507 database. This assessment makes use of a recent, improved description of the ternary Al-Fe-Si system. In the present work, modeling of the Al-rich corner of the quaternary Al-Fe-Mn-Si system has been carried out by introducing Fe solubility into the so-called alpha-AlMnSi and beta-AlMnSi phases of the Al-Mn-Si system. A critical review of the data available on the quaternary system is presented and used for the extension of the description of these ternary phases into the quaternary Al-Fe-Mn-Si.

DOI: 10.1007/s11661-010-0263-x

I. INTRODUCTION

CHECKING for additions and impurities in cast Al-Si aluminum alloys becomes more and more important as the use of scrap materials increases. Among the most common impurities is iron, which may lead to the precipitation of various phases, either stable or metastable.[1] Figure 1(a) shows the liquidus projection in the aluminum corner of the stable ternary Al-Fe-Si system according to a recent reassessment.[2] In addition to the Al-rich (Al) solid solution and to Si, four compounds noted gamma-τ_2, delta-τ_4, alpha-τ_5, and beta-τ_6 are shown in this figure. Table I lists the crystallographic structure and the chemical formula of these phases. As will be briefly described in Section I–A, the reassessment was based on the COST-507 database[3] and limited to changes in the description of the compounds in order to describe the solubility range of each one of them.

Among the other beneficial effects, manganese is added to Al-Si alloys, containing iron, in order to avoid precipitation of the beta-τ_6 phase that often forms as elongated plates, thus decreasing the mechanical properties of the cast parts. Such a solution has been applied for a long time to improve the quality of cast parts but should be mastered through the appropriate description of phase equilibria in the Al-Fe-Mn-Si system. Figure 1(b) presents the Al-rich corner of the liquidus projection of the Al-Mn-Si system as calculated using the COST-507 database, the features of which have been confirmed by a more recent experimental study of the entire phase diagram.[35] Two ternary compounds show up in the Al-rich corner that are denoted alpha-AlMnSi and beta-AlMnSi (Table I for their structure). The alpha-AlMnSi phase has a very limited composition domain corresponding to the formula, Al_9Mn_2Si, while the beta-AlMnSi phase extends significantly around the composition $(Al,Si)_{10}Mn_3$.[35] Substitution of Si to Al has been studied in both alpha-AlMnSi[10] and beta-AlMnSi[11] phases. For the assessment of the system limited to the Al-rich corner, a description of both phases, as line compounds with cross-substitution of Al and Si, was adopted in the COST-507 database, as shown in Table I.

The most noteworthy work on the Al-rich corner of the quaternary Al-Fe-Mn-Si system is from Phillips and Varley,[4] who performed an extensive study using thermal analysis and optical microscopy. They reported isopleth sections showing microstructure maps, indicating the phases formed in slowly cooled samples with Si, Mn, and Fe contents varying from 0 to 4 wt pct. While Phillips and Varley,[4] and later Phragmen,[5] did not differentiate the alpha-AlMnSi and alpha-τ_5 phases, Munson[6] and Sun and Mondolfo[7] showed, through X-ray examination, that alpha-AlMnSi is simple cubic and alpha-τ_5 is hexagonal. These are thus two different phases so that there cannot be one single-phase field from the alpha-AlMnSi phase field in the Al-Mn-Si system to the alpha-τ_5 field in the Al-Fe-Si system. Following the work by Munson,[6] Barlock and Mondolfo[8] observed that the alpha-AlMnSi phase extends deeply into the quaternary system, almost reaching the ternary Al-Fe-Si, with up to 85 pct of Mn atoms being substituted by Fe atoms. Davignon *et al.*[9] determined a four-phase equilibrium at 823 K (550 °C) involving (Al), Si, alpha-AlMnSi, and beta-τ_6 phases. The composition of these phases was determined using electron probe microanalysis, which confirms the large solubility of Fe in the alpha-AlMnSi phase. On the other hand, the solubility of Mn in the compounds of the Al-Fe-Si system is not well known, but it seems to be established that it is lower than 0.5 at. pct for the alpha-τ_5 and beta-τ_6 phases according to Du *et al.*[21]

JACQUES LACAZE, Senior Scientist, is with CIRIMAT, Université de Toulouse, ENSIACET, BP 44362, 31432 Toulouse Cedex 4, France. Contact e-mail: jacques.lacaze@ensiacet.fr LUIZ ELENO, Postdoctoral Student, formerly with CIRIMAT, Université de Toulouse, is with the Departamento de Engenharia Metalúrgica e de Materiais, Escola Politécnica da Universidade de São Paulo, Av. Prof. Mello Morais, 2463, 05508-030 São Paulo, SP, Brasil. BO SUNDMAN, Visiting Researcher, formerly with CIRIMAT, Université de Toulouse, is with INSTN, CEA Saclay, 91190 Gif sur Yvette Cedex, France.

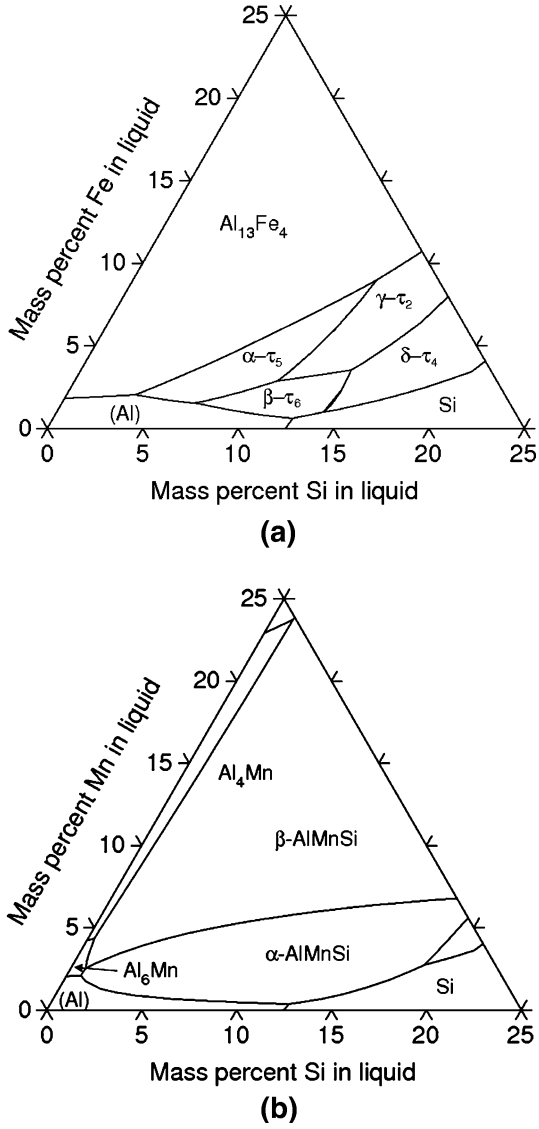

Fig. 1—Calculated liquidus projection of the aluminum corner of the (*a*) Al-Fe-Si[2] and (*b*) Al-Mn-Si[3] systems.

In addition to the alpha-AlMnSi phase, Phillips' and Varley's work[4] suggests that the beta-AlMnSi phase also extends deeply in the quaternary system, and this should be associated with Mn substitution by Fe. Very little has been found in the literature concerning this latter phase, but a high Fe solubility has been reported by Brandt *et al.*[15] In this work, up to 28 pct of Mn atoms could be substituted with Fe atoms in the beta-AlMnSi phase. In the case of the alpha-AlMnSi phase, a slight decrease in Si content with increase in Fe has been reported.[14,28] However, the most important effect of substituting Fe for Mn is in the crystallographic structure of the alpha-AlMnSi, which has been investigated several times.[12–14] An order-disorder reaction seems to take place within the stability range of the alpha-AlMnSi phase, which changes from a simple cubic to a body-centered-cubic structure with increasing Fe content.[13,14] Davignon *et al.*[9] suggested that the reaction has a second-order character; thus, no two-phase field should separate both variants of the phase. To sum up, the various works presented previously suggest that the alpha-AlMnSi and beta-AlMnSi phases extend significantly within the Al-Fe-Mn-Si system and that no new quaternary phase appears in the aluminum corner.

This view of the Al-rich corner of the quaternary Al-Fe-Mn-Si system has been contradicted by Zakharov *et al.*[16] These authors investigated alloys with 2 wt pct Fe, 10 and 14 wt pct Si, and 0 to 4 wt pct Mn, and detected the presence of an fcc quaternary phase with a formula presented as $Al_{16}(Mn,Fe)_4Si_3$. Likewise, Flores *et al.*[17] and Onderka *et al.*[18] looked to refine aluminum alloys by precipitating a compound that was defined either as $Al_8FeMnSi_2$[17] or $Al_{11.8}FeMn_{1.6}Si_{1.6}$,[18] the structures of which were, unfortunately, not investigated. However, in a parallel study on sintering quaternary alloys with 14.6 wt pct Fe, 14.3 wt pct Mn, and 14.7 wt pct Si, Toscano *et al.*[19] only found the cubic alpha-AlMnSi and the hexagonal beta-AlMnSi phases. It thus seems that up to now, only one experimental work[16] has reported the existence of a stable quaternary phase in the composition range where the alpha-AlMnSi phase is observed.

Perhaps because *this* eases compatibility with previous lower-order assessments, all published thermodynamic modeling studies of the quaternary Al-Fe-Mn-Si system assumed the existence of such a quaternary phase. Balitchev *et al.*[20] used the COST-507 database and accepted the results of Zakharov *et al.*[16] to fit the parameters of the assumed quaternary phase. Both Du *et al.*[21] and Abou and Malakhov[22] compared their simulations with new experimental results on A356.1 and AA6111 alloys, respectively. Moreover, neither of these two works gives any experimental evidence that a phase differing from Fe-bearing alpha-AlMnSi was observed. *Ab-initio* calculations, such as those performed by Ravi and Wolverton[23] in their comparison of available databases for aluminum alloys, could certainly be decisive in confirming the existence of such a quaternary phase. Unfortunately, such data are unavailable for the phases discussed here.

Due to this lack of evidence concerning the existence of a separate quaternary phase, it was decided to rely upon the view of Munson[6] and Barlock and Mondolfo,[8] *i.e.*, that the alpha-AlMnSi phase extends deeply into the quaternary system, almost reaching the ternary Al-Fe-Si, and that there is no stable quaternary phase in the aluminum corner of the Al-Fe-Mn-Si system. This is, in fact, in agreement with the recent conclusions of Belov *et al.*[24] The starting point for the present thermodynamic optimization was the COST-507 database,[3] together with a recent reoptimization of the Al-Fe-Si system.[2] The models for the alpha-AlMnSi and beta-AlMnSi phases have been modified in order to allow for substitution of Mn by Fe.

A. *Thermodynamic Modeling*

The original COST-507 database contained the description of the four compounds appearing in

Table I. Crystallographic Structure, Model, and Thermodynamic Parameters of the Phases in the Ternary Al-Fe-Si System[2] and of the Two Compounds of the Al-Mn-Si System; the Most Common Formula of the Al-Fe-Si Compounds Has Been Indicated Together with the Name Used in the Present Work

Phase	Structure	Model	Parameters
Alpha-τ_5 (Al_8Fe_2Si)	hexagonal	$Al_{0.6612}Fe_{0.19}Si_{0.0496}(Al,Si)_{0.0992}$	$G^{alpha-\tau5}_{Al:Fe:Si:Al} - 0.7604.^\circ G^{fcc}_{Al} - 0.19.^\circ G^{bcc}_{Fe} - 0.0496.^\circ G^{dia}_{Si} = -28,100 + 9.1.T$ $G^{alpha-\tau5}_{Al:Fe:Si:Si} - 0.6612.^\circ G^{fcc}_{Al} - 0.19.^\circ G^{bcc}_{Fe} - 0.1488.^\circ G^{dia}_{Si} = -25,310 + 5.0.T$
Beta-τ_6 (Al_5FeSi)	monoclinic	$Al_{0.598}Fe_{0.152}Si_{0.10}(Al,Si)_{0.15}$	$G^{beta-\tau6}_{Al:Fe:Si:Al} - 0.748.^\circ G^{fcc}_{Al} - 0.152.^\circ G^{bcc}_{Fe} - 0.10.^\circ G^{dia}_{Si} = -26,900 + 12.T$ $G^{beta-\tau6}_{Al:Fe:Si:Si} - 0.598.^\circ G^{fcc}_{Al} - 0.152.^\circ G^{bcc}_{Fe} - 0.25.^\circ G^{dia}_{Si} = -19,800 + 3.T$
Gamma-τ_2 ($Al_5Fe_2Si_2$)	monoclinic	$Al_{0.5}Fe_{0.2}Si_{0.1}(Al,Si)_{0.2}$	$G^{gamma-\tau2}_{Al:Fe:Si:Al} - 0.70.^\circ G^{fcc}_{Al} - 0.20.^\circ G^{bcc}_{Fe} - 0.10.^\circ G^{dia}_{Si} = -27,300 + 6.8.T$ $G^{gamma-\tau2}_{Al:Fe:Si:Si} - 0.50.^\circ G^{fcc}_{Al} - 0.20.^\circ G^{bcc}_{Fe} - 0.30.^\circ G^{dia}_{Si} = -28,700 + 8.0.T$
Delta-τ_4 (Al_3FeSi_2)	tetragonal	$Al_{0.4166}Fe_{0.1667}Si_{0.25}(Al,Si)_{0.1667}$	$G^{delta-\tau4}_{Al:Fe:Si:Al} - 0.5833.^\circ G^{fcc}_{Al} - 0.1667.^\circ G^{bcc}_{Fe} - 0.25.^\circ G^{dia}_{Si} = -18,100$ $G^{delta-\tau4}_{Al:Fe:Si:Si} - 0.4166.^\circ G^{fcc}_{Al} - 0.1667.^\circ G^{bcc}_{Fe} - 0.4167.^\circ G^{dia}_{Si} = -24,700 + 7.0.T$
Liquid			$L^{liquid}_{Al,Fe,Si} = -110,000 + 100.0.T$
Alpha-AlMnSi	cubic	$Al_{16}(Fe,Mn)_4Si_1(Al,Si)_2$	$G^{alpha-AlMnSi}_{Al:Mn:Si:Al} - 18.^\circ G^{fcc}_{Al} - 4.^\circ G^{cbcc}_{Mn} -^\circ G^{dia}_{Si} = -551,382 + 250.225.T$ $G^{alpha-AlMnSi}_{Al:Mn:Si:Si} - 16.^\circ G^{fcc}_{Al} - 4.^\circ G^{cbcc}_{Mn} - 3.^\circ G^{dia}_{Si} = -525,358 + 167.895.T$ $G^{alpha-AlMnSi}_{Al:Fe:Si:Al} - 18.^\circ G^{fcc}_{Al} - 4.^\circ G^{bcc}_{Fe} -^\circ G^{dia}_{Si} = -785,324 + 402.33.T$ $G^{alpha-AlMnSi}_{Al:Fe:Si:Si} - 16.^\circ G^{fcc}_{Al} - 4.^\circ G^{bcc}_{Fe} - 3.^\circ G^{dia}_{Si} = -716,300 + 320.T$
Beta-AlMnSi	hexagonal	$Al_{15}Si_1(Al,Si)_4(Mn,Fe)_6$	$G^{beta-AlMnSi}_{Al:Si:Al:Fe} - 19.^\circ G^{fcc}_{Al} - 6.^\circ G^{cbcc}_{Fe} -^\circ G^{dia}_{Si} = -557,000$ $G^{beta-AlMnSi}_{Al:Si:Si:Fe} - 15.^\circ G^{fcc}_{Al} - 6.^\circ G^{cbcc}_{Fe} - 5.^\circ G^{dia}_{Si} = -448,114 - 164.3488.T$ $G^{beta-AlMnSi}_{Al:Si:Al:Mn} - 19.^\circ G^{fcc}_{Al} - 6.^\circ G^{cbcc}_{Mn} -^\circ G^{dia}_{Si} = -679,423 + 225.809.T$ $G^{beta-AlMnSi}_{Al:Si:Si:Mn} - 15.^\circ G^{fcc}_{Al} - 6.^\circ G^{cbcc}_{Mn} - 5.^\circ G^{dia}_{Si} = -570,537 + 61.4602.T$

Figure 1(a) for the Al-Fe-Si system. As emphasized in the reassessment of the Al-rich corner of this system,[2] all of these compounds are known experimentally as line compounds with substitution of Al and Si. The model for the alpha-τ_5 phase was kept the same as in the COST-507 database, since it was already described as a line compound. Liu and Chang's model[25] was employed for the beta-τ_6 phase, while for the gamma-τ_2 and delta-τ_4 phases, stoichiometry was chosen to match observed composition ranges, *i.e.*, the known substitution range of Si for Al. Table I lists the model adopted for each of these compounds and the value of the optimized coefficients of the Gibbs energy function for each of the phases. The ideal solution model was used for the four line compounds. All other phases of the databank were kept the same as in the COST-507 database, apart from the liquid phase to which a ternary interaction parameter (that is also given in Table I) was added. The composition ranges of all four compounds could thus match the available experimental information[2] well, in close alignment with recent results on the Al-Fe-Si system.[26,27]

The models for the alpha-AlMnSi and beta-AlMnSi phases from the COST-507 database have been changed with the introduction of Fe solubility in the Mn sublattice. The model adopted for these phases is therefore $Al_{16}Si_1(Al,Si)_2(Fe,Mn)_4$ and $Al_{15}Si_1(Al,Si)_4(Fe,Mn)_6$, respectively. No attempt was made to model the order-disorder transition within the alpha-AlMnSi stability range or the slight decrease in Si content in this phase with the increase in Fe, as observed experimentally.[14,28]

Table II. Invariant Equilibria Involving the Liquid in the Al-Rich Corner of the Al-Fe-Mn-Si System: Experimental Results[4] in Bold Font are Compared to Calculated Data in Normal Font

Phases Present	Temperature
$Al_{13}Fe_4$, Al_6Mn, alpha-AlMnSi, (Al)	**648**/643
Beta-τ_6, alpha-AlMnSi, Si, (Al)	**575**/576
$Al_{13}Fe_4$, Al_4Mn, Al_6Mn, beta-AlMnSi	**731**/754
$Al_{13}Fe_4$, Al_6Mn, alpha-AlMnSi, beta-AlMnSi	**695**/699

B. *Optimization*

Phillips and Varley[4] determined four invariant reactions in the Al-rich corner of the Al-Fe-Mn-Si system, giving the temperature and approximate values for the corresponding liquid compositions. From preliminary calculations, it was inferred that the alpha phase observed by Phillips and Varley in three of these equilibria should be the alpha-AlMnSi phase. These four invariant equilibria are listed in Table II along with the corresponding experimental temperatures that were used for optimization. The calculated temperatures are also listed.

Davignon *et al.*[9] determined the composition of the alpha-AlMnSi and beta-τ_6 phases present in a four-phase equilibrium with (Al) and Si at 550 °C. These data were important to optimize Fe substitution for Mn in the alpha-AlMnSi phase. They are listed in Table III together with the values calculated after optimization.

A number of liquidus values for the alpha-AlMnSi phase were read from the isopleth sections by Phillips

and Varley.[4] As already mentioned by Du *et al.*,[21] the liquidus values in the experimental isopleth sections sometimes match only poorly the values assessed for the limiting ternaries. This may be due to extensive undercooling before solidification experienced during thermal analysis, and it was thus decided to increase all the experimental liquidus values by 20 °C, as already done by Du *et al.*[21] Table IV lists the data entered for optimization as well as the calculated values.

Finally, 3 three-phase equilibria were considered to optimize the parameters of the beta-AlMnSi phase and are listed in Table V. In each case, two solute contents were fixed while the temperature and the content in the third solute were used as experimental data. Once again, the values calculated at the end of the optimization are also listed in the table.

The PARROT module of the Thermocalc software[29] was used for the evaluation of the model parameters, the values of which are given in Table I.

II. RESULTS AND DISCUSSION

Comparing calculated values with experimental ones used for optimization (Tables I through 5) shows a satisfactory description of the phases in the Al corner of the Al-Fe-Mn-Si systems. The entire set of vertical sections from Philips and Varley[4] were then used to check the quality of the parameters obtained. According to Phillips and Varley,[4] any phase formed in the course of solidification (either primary or resulting from eutectic or peritectic transformation) is expected to be inherited in the final microstructure. Because of this, and also because of microsegregation buildup, microstructure maps may differ greatly from the corresponding stable isopleths sections. Accordingly, the liquidus is the only part of the calculated isopleth sections that should be compared with data in the microstructure maps. When the comparison was limited to the liquidus, a good agreement was observed between calculated and experimental sections (Figures 2 and 3).

Figure 2 (respectively, Figure 3) compares the calculated isopleth section for $w_{Fe} = 1$ wt pct and $w_{Mn} = 3$ wt pct (respectively, $w_{Mn} = 1$ wt pct and $w_{Si} = 3$ wt pct) to the corresponding microstructure map provided by Phillips and Varley.[4] The experimental liquidus appeared to be too low, and this is reflected in the shift to higher temperatures of most of the calculated liquidus in Figures 2 and 3 when compared to the experimental ones.

Apart from this difference, the shape of the calculated and experimental liquidus in Figure 2 is quite similar and the three primary phase fields, for the phases Al_6Mn, beta-AlMnSi, and alpha-AlMnSi, are observed to be present in both diagrams. The primary phase field for the beta-AlMnSi phase appears to extend much more toward higher silicon contents in the experimental than in the calculated diagram; this may be related to higher undercoolings for nucleation of the alpha-AlMnSi phase, as suggested with the corresponding lower liquidus temperatures. The formation of the (Al) phase also appears at very similar temperatures in both diagrams.

For the composition range of the alloys corresponding to Figure 2, the silicon phase precipitates only during the eutectic reactions at about 575 °C. As expected from the buildup of microsegregation during solidification, the silicon phase is observed experimentally to appear at much lower silicon contents than according to the stable phase diagram. This is also related to a much larger extension to lower silicon contents of the fields with liquid at intermediate temperatures in Figure 2(b) as compared to Figure 2(a). Microsegregation and limited solid-state homogenization during solidification are also the reason for the presence of the additional vertical lines in the experimental diagram, which is due to the inheritance of the phases, as described previously. As a matter of fact, such features could be calculated with Scheil's model, which assumes there is no solid-state diffusion during solidification, as previously illustrated in the case of Al-Cu-Mg-Si[30] and Al-Fe-Mn-Si[31] aluminum alloys.

Table III. Four-Phase Equilibrium at 550 °C; Comparison of Experimental Composition (Atomic Percent) of the Phases[9] in Bold Font with Calculated Values in Normal Font

Phase	Fe	Mn	Si
(Al)	**0**/0.001	**0**/0.008	**0**/1.2
Si	**0**/0	**0**/0	**100**/100
Alpha-AlMnSi	**11.8**/12.4	**4.0**/5.0	**10.6**/10.4
Beta-τ_6	**12.8**/15.2	**0.4**/0	**18.1**/18.66

Table IV. Comparison of Experimental Liquidus Values of the Alpha-AlMnSi Phase[4] Used for Optimization with the Calculated Values

w_{Fe} (Wt pct)	w_{Mn} (Wt pct)	w_{Si} (Wt pct)	Experimental (°C)	Calculated (°C)
2	2	1.5	698	682
2	2	2.0	694	686
2	2	3.0	690	691
2	2	4.0	691	693
1	1	4.0	659	654
1	2	4.0	675	685
1	3	4.0	682	707
1	3	3.0	697	704
2	3	3.0	697	710
3	3	3.0	704	716

Table V. Data Used for Optimizing the Parameters of the Beta-AlMnSi Phase

Phases	Fixed Compositions	Experimental Values	Calculated Values
$Al_{13}Fe_4$, beta-AlMnSi	$w_{Mn} = 0.04$, $w_{Si} = 0.02$	737 °C, $w_{Fe} = 0.03$	747 °C, $w_{Fe} = 0.032$
Al_6Mn, beta-AlMnSi	$w_{Fe} = 0.02$, $w_{Si} = 0.01$	697 °C, $w_{Mn} = 0.03$	728 °C, $w_{Mn} = 0.039$
Alpha-AlMnSi, beta-AlMnSi	$w_{Fe} = 0.01$, $w_{Si} = 0.04$	687 °C, $w_{Mn} = 0.035$	716 °C, $w_{Mn} = 0.0035$

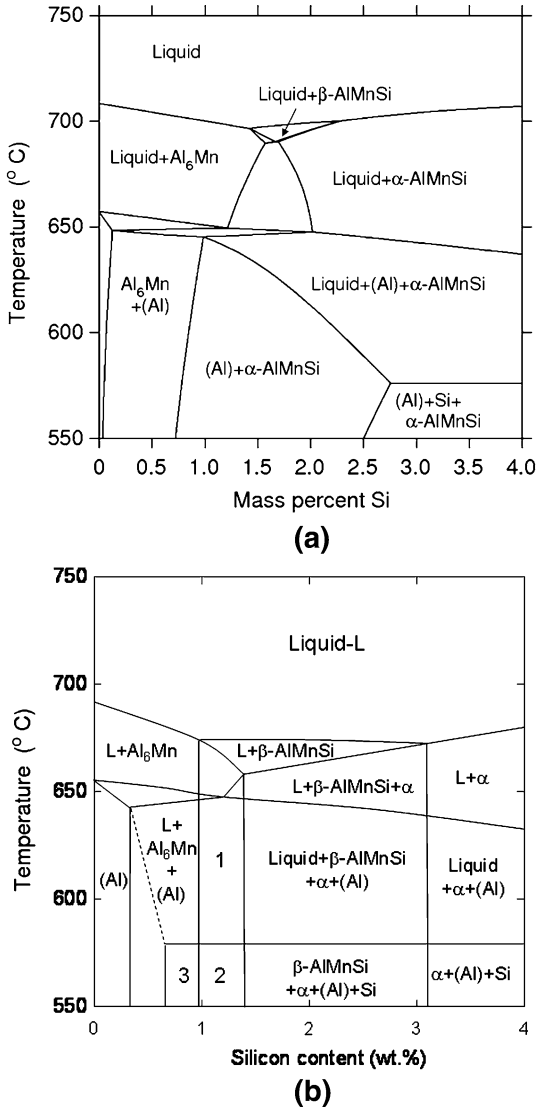

Fig. 2—Comparison of the calculated isopleth section at $w_{Fe} = 1$ wt pct and $w_{Mn} = 3$ wt pct of (*a*) the stable phase diagram with (*b*) the corresponding experimental microstructure map.[4] The numbers refer to the following phase fields: (1) liquid + beta-AlMnSi + (Al) + alpha-AlMnSi, (2) beta-AlMnSi + (Al) + alpha-AlMnSi + (Al) + Si, and (3) beta-AlMnSi + Al_6Mn + (Al) + Si. In (b), the name alpha was kept in agreement with the original work by Phillips and Varley,[4] though they did not differentiate τ_5 and alpha-AlMnSi phases.

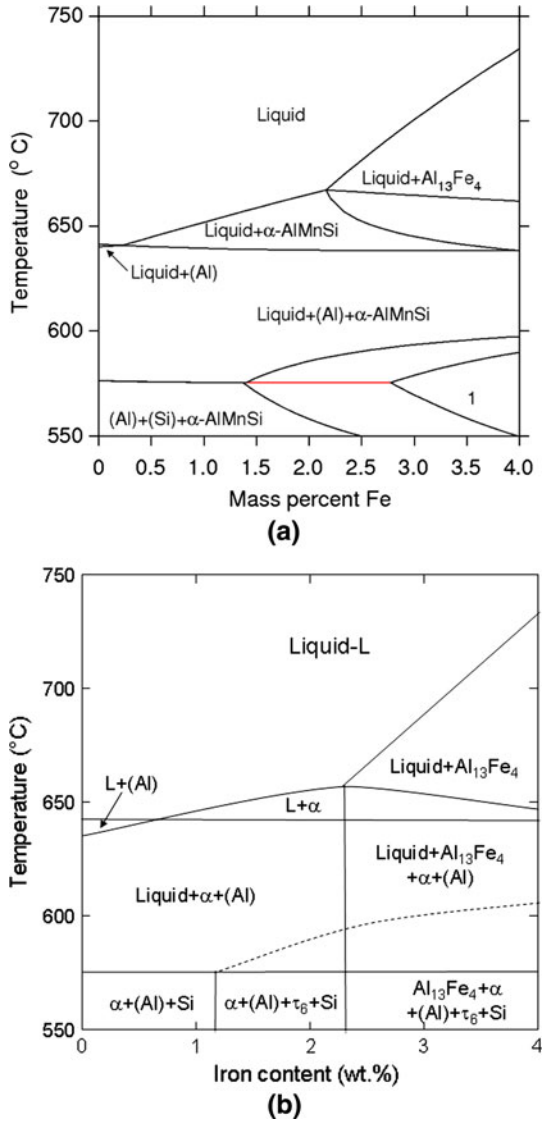

Fig. 3—Comparison of (*a*) the calculated isopleth section at $w_{Mn} = 1$ wt pct and $w_{Si} = 3$ wt pct of the stable phase diagram (*b*) with the experimental microstructure map.[4] The number (1) refers to the following phase field: alpha-AlMnSi + (Al) + $Al_{13}Fe_4$. In (b), the name alpha was kept in agreement with the original work by Phillips and Varley,[4] though they did not differentiate τ_5 and alpha-AlMnSi phases.

The isopleth section shown in Figure 3 was selected, because this is the one that was used by Du *et al.*[21] to illustrate their optimization. As seen in Figure 3, the liquidus calculated with the present assessment agrees fairly well with the experimental one. It is also noticed that the formation of the beta-τ_6 phase appears at similar iron contents and temperatures in both diagrams (dotted line in Figure 3(b)). As previously discussed, Si was observed experimentally to precipitate in a much larger Fe domain than calculated at equilibrium. In contrast, the section calculated by Du *et al.*[21] shows many more lines in between the temperatures for (Al) and Si precipitation, only part of them being related to the precipitation of the added quaternary phase. Not only did these lines not show up as thermal arrests in the experimental study,[4] but according to Scheil's calculation, they would also lead to discrepancies between predicted and experimental microstructures.

The list of invariant reactions in the quaternary system involving the liquid phase assessed by Phillips and Varley[4] and given in Table II was extended by Mondolfo.[32] The six quaternary invariant equilibria listed by Mondolfo are reproduced in Table VI, using the same labels that this author used for four of the equilibria (first column of Table VI). Note that Mondolfo took the four equilibria listed by Phillips and Varley, but a typing error, which appeared in his work,[32] has here been corrected: in the last line of

Table VI. List of Quaternary Invariant Points Involving the Liquid, in Bold, According to Mondolfo[32] and in Normal Font as Calculated in the Present Work; the References in the First Column Refer to Mondolfo[32]

Reference	Phases Present	Temperature (°C)	w_{Fe} (Wt pct)	w_{Mn} (Wt pct)	w_{Si} (Wt pct)
J	liquid + $Al_{13}Fe_4$ + Al_6Mn → alpha-AlMnSi + (Al)	**648**/643	**2.00**/1.6	**0.35**/0.6	**1.75**/2.0
K	liquid + $Al_{13}Fe_4$ → alpha-AlMnSi + τ_5 + (Al)	**627 to 632**	**2 to 2.5**	**<0.2**	**3 to 5**
L	liquid + τ_5 + $Al_{13}Fe_4$ → alpha-AlMnSi + τ_6 + (Al)	**597 to 607**	**1 to 2**	**0.1 to 0.5**	**5 to 10**
M	liquid + τ_6 → alpha-AlMnSi + Si + (Al)	**575**/576	**0.6**/0.6	**0.2**/0.2	**11.7**/12.6
	$Al_{13}Fe_4$, Al_4Mn, Al_6Mn, beta-AlMnSi	**729**/754	**2.35**/2.5	**3.9**/5.3	**0.35**/0.5
	$Al_{13}Fe_4$, Al_6Mn, alpha-AlMnSi, beta-AlMnSi	**695**/699	**2.35**/2.3	**2.60**/2.4	**1.35**/2.2

Table VI, the alpha-AlMnSi phase is substituted for beta-τ_6 (or Fe_2AlSi_8). The table shows the assessed values (in bold) and the ones calculated according to the present optimization (in normal font), apart for invariant points K and L. Because no manganese solubility was considered in the τ_5 and τ_6 phases, these latter two points were, in fact, calculated to be very close to the related Al-Fe-Si ternary invariants (without the alpha-AlMnSi phase). For the four other invariant points that are the most important for practical applications, the agreement between calculated and assessed values is seen to be highly satisfactory.

The general agreement between experimental and calculated diagrams illustrated in Figures 2 and 3 supports the choice made for the present study that no quaternary phase appears in the Al-rich corner of the Al-Fe-Mn-Si phase diagram. However, it appeared of interest to attempt to compare the present calculations with the two experimental sections reported by Zakharov *et al.*[16] Figure 4 shows the corresponding sections calculated using the present assessment. The general shape of these sections corresponds well to the experimental ones, except for the additional lines in the experimental sections that have been added to the present graphs as dotted and interrupted lines.

In both calculated sections in Figure 4, the liquidus is dominated by the primary phase field of the alpha-AlMnSi phase, when this is the assumed quaternary phase that shows up in the experimental sections.[16] According to Zakharov *et al.*,[16] the alpha-AlMnSi phase was observed to form at much lower temperature as represented by the interrupted line in both graphs of Figure 4. By introducing the assumed quaternary phase and limiting the amount of Fe that can be substituted for Mn in the alpha-AlMnSi phase, both Balitchev *et al.*[20] and Abou and Malakhov[22] were able to reproduce these experimental figures.

At a lower temperature, the nearly horizontal calculated lines in Figure 4 around 600 °C and 575 °C relate to the precipitation of (Al) and Si, respectively, in the section at 10 wt pct Si (Figure 4(a)) and Si and (Al), respectively, in the section at 14 wt pct Si (Figure 4(b)). These two lines agree with the experimental report in the case of the 10 wt pct Si section, as well as with the calculations of both Balitchev *et al.*[20] and Abou and Malakhov.[22] On the contrary, precipitation of Si was found experimentally at a much higher temperature in

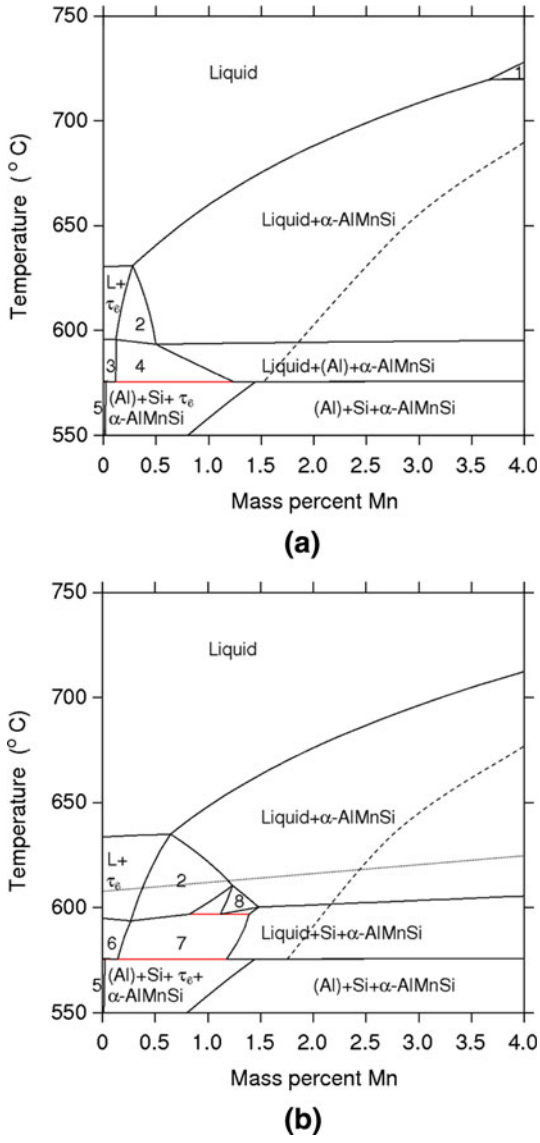

Fig. 4—Calculated isopleth sections for (*a*) w_{Fe} = 2 wt pct and w_{Si} = 10 wt pct or (*b*) 14 wt pct, corresponding to those produced experimentally by Zakharov *et al.*[16] The dotted and interrupted lines are the main lines missing in the calculations and present in the experimental sections. The numbers refer to the following phase fields: (1) liquid + beta-AlMnSi, (2) liquid + τ_6 + alpha-AlMnSi, (3) liquid + τ_6 + (Al), (4) liquid + τ_6 + (Al) + alpha-AlMnSi, (5) τ_6 + Si + (Al), (6) liquid + τ_6 + Si, (7) liquid + τ_6 + Si + alpha-AlMnSi, and (8) liquid + τ_4 + alpha-AlMnSi.

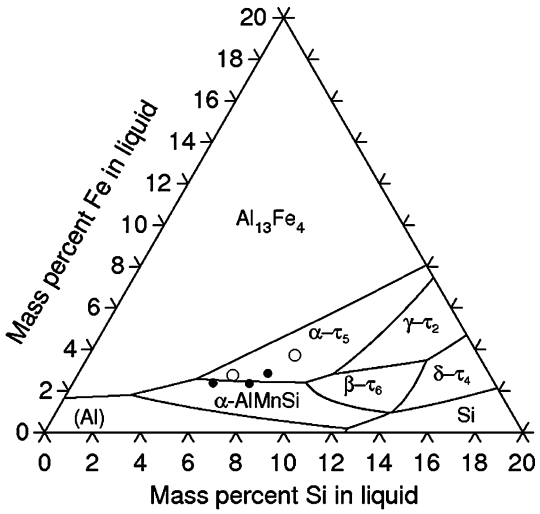

Fig. 5—Section of the liquidus projection of the Al-Fe-Mn-Si system at 0.3 wt pct Mn. Experimental points from Munson[6] have been added, with circles and disks showing, respectively, compositions for which alpha-τ_5 or alpha-AlMnSi is the primary phase.

the section at 14 wt pct Si, as indicated by the dotted line in Figure 4(b). While Balitchev *et al.*[20] did not show their calculations for that silicon content, Abou and Malakhov's[22] results were similar to those found in the current study, *i.e.*, precipitation of Si at temperatures close to 600 °C at 14 wt pct Si. Accordingly, the dotted line in Figure 4(b) remains unexplained, even by assessments based on these experimental results. Along with the conclusions of the review presented in Section I, this shows the need for further experiments before rejecting the view proposed long ago and adopted in the present work that no quaternary phase appears in the Al-rich corner of the Al-Fe-Mn-Si phase diagram and that the alpha-AlMnSi and beta-AlMnSi phases extend significantly from the Al-Mn-Si system within the quaternary.

The present optimization was finally used to calculate the section of the liquidus projection of the Al corner of the quaternary Al-Fe-Mn-Si system at 0.3 wt pct Mn for comparison with the experimental section proposed by Munson.[6] The few data points used by these authors were located along the boundary between the alpha-AlMnSi and the alpha-τ_5 phases, while all other boundaries were drawn with dashed lines to highlight the lack of information. Comparing Figure 5 with the drawing by Munson shows a very good agreement for the alpha-AlMnSi/alpha-τ_5 boundary, while the present calculation shows much more complicated features than anticipated by Munson for the rest of the diagram. In particular, the delta-τ_4 phase of the Al-Fe-Si system is stabilized by Mn, as suggested by its observation in as-cast Al-Si alloys[33] and in resolidified brazing.[34]

III. CONCLUSIONS

Starting from the COST-507 database, which is the reference for thermodynamic properties of aluminum alloys based on the description of ternary systems, a CALPHAD-type assessment of the quaternary Al-Fe-Mn-Si system has been proposed. There are contradictory results in the literature as to the existence of a quaternary phase, and the thermodynamic assessment has showed that more experimental information is needed before confirming the existence of such a phase. The present work has allowed us to satisfactorily reproduce most of the experimental features available for the aluminum corner of the Al-Fe-Mn-Si system by accounting for significant substitution of Mn by Fe in the two relevant ternary compounds of the Al-Mn-Si system, the so-called alpha-AlMnSi and beta-AlMnSi phases.

ACKNOWLEDGMENT

Financial support from ESA (MICAST MAP project) is greatly acknowledged.

REFERENCES

1. G. Ghosh: *Ternary Alloys, a Comprehensive Compendium of Evaluated Constitutional Data and Phase Diagrams*, G. Petzow and G. Effenberg, eds., VCH Publishers, New York, NY, 1992, vol. 5, pp. 394–438.
2. L. Eleno, J. Vezelý, B. Sundman, M. Cieslar, and J. Lacaze: *Mater. Sci. Forum*, 2010, vol. 649, pp. 523–28.
3. I. Ansara, A.T. Dinsdale, and M.H. Rand: *COST-507—Thermochemical Database for Light Metal Alloys*, European Commission, Brussels, Belgium, 1998.
4. H.W.L. Phillips and P.C. Varley: *J. Inst. Met.*, 1943, vol. 69, pp. 317–50.
5. G. Phragmen: *J. Inst. Met.*, 1950, vol. 77, pp. 489–552.
6. D. Munson: *J. Inst. Met.*, 1967, vol. 95, pp. 217–19.
7. C.Y. Sun and L.F. Mondolfo: *J. Inst. Met.*, 1967, vol. 95, p. 384.
8. J.G. Barlock and L.F. Mondolfo: *Z. Metallkd.*, 1975, vol. 66, pp. 605–11.
9. G. Davignon, A. Serneels, B. Verlinden, and L. Delaey: *Metall. Mater. Trans. A*, 1996, vol. 27A, pp. 3357–61.
10. J.E. Tibbals: *Key Eng. Mater.*, 1990, vols. 44–45, pp. 233–46.
11. L.A. Bendersky, J.W. Cahn, and D. Gratias: *Phil. Mag. B*, 1989, vol. 60, pp. 837–54.
12. Z.H. Lai and C.H. Li: *Scripta Metall. Mater.*, 1993, vol. 29, pp. 895–900.
13. P. Donnadieu, G. Lapasset, and T.H. Sanders: *Phil. Mag. Lett.*, 1994, vol. 70, pp. 319–26.
14. N. Krendelsberger: Ph.D. Thesis, Innovative Materials Group, Universität Wien, Vienna, 2001.
15. R.A. Brandt, G. Le Caër, J.M. Dubois, F. Hippert, C. Sauer, and J. Pannetier: *J. Phys.: Condens. Matter*, 1990, vol. 2, pp. 3855–65.
16. A.M. Zakharov, I.T. Gul'din, A.A. Arnol'd, and Y.A. Matsenko: *Russ. Metall.*, 1989, vol. 4, pp. 209–13.
17. A. Flores, M. Sukiennik, A.H. Castillejos, F.A. Acosta, and J.C. Escobedo: *Intermetallics*, 1998, vol. 6, pp. 217–27.
18. B. Onderka, M. Sukiennik, and K. Fitzner: *Arch. Metall.*, 2000, vol. 45, pp. 119–32.
19. J.A.G. Toscano, A.V. Flores, A.R. Salina, and E.V. Nava: *Mater. Lett.*, 2003, vol. 57, pp. 2246–52.
20. E. Balitchev, T. Jantzen, I. Hurtado, and D. Neuschütz: *CALPHAD*, 2003, vol. 27, pp. 275–78.
21. Y. Du, Y.A. Chang, S. Liu, B. Huang, F.-Y. Xie, Y. Yang, and S.L. Chen: *Z. Metallkd.*, 2005, vol. 96, pp. 1351–62.
22. M.K. Abou Khatwa and D.V. Malakhov: *CALPHAD*, 2006, vol. 30, pp. 159–70.
23. C. Ravi and C. Wolverton: *Metall. Mater. Trans. A*, 2005, vol. 36A, pp. 2013–23.

24. N.A. Belov, D.G. Eskin, and A.A. Aksenov: *Multicomponent Phase Diagrams: Applications for Commercial Aluminium Alloys*, Elsevier, New York, NY, 2005, p. 19.
25. Z.-K. Liu and Y.A. Chang: *Metall. Mater. Trans. A*, 1999, vol. 30A, pp. 1081–95.
26. S. Pontevichi, F. Bosselet, O. Dezellus, M. Peronnet, D. Rouby, and J.C. Viala: *J. Phys. IV France*, 2004, vol. 113, pp. 81–84.
27. N. Krendelsberger, F. Weitzer, and J.C. Schuster: *Metall. Mater. Trans. A*, 2007, vol. 38A, pp. 1681–91.
28. J.E. Tibbals, J.A. Horst, and C.J. Simensen: *J. Mater. Sci.*, 2001, vol. 36, pp. 937–41.
29. J.-O. Andersson, T. Helander, L. Höglund, P. Shi, and B. Sundman: *CALPHAD*, 2002, vol. 26, pp. 273–12.
30. J. Lacaze and G. Lesoult: in *State of the Art of Computer Simulation of Casting and Solidification Processes*, H. Fredriksson, ed., Les Editions de Physique, Les Ulis, France, 1986, pp. 119–27.
31. L. Eleno, B. Sundman, and J. Lacaze: in *Modelling of Casting, Welding and Advanced Solidification Processes—XII*, L. Cockcroft and D.M. Maijer, eds., Vancouver TMS, Warrendale, PA, 2009, pp. 635–42.
32. L.F. Mondolfo: *Aluminium Alloys: Structure and Properties*, Butterworths, Boston, MA, 1976, pp. 658–60.
33. M.V. Kral: *Mater. Lett.*, 2005, vol. 59, pp. 2271–76.
34. M. Dehmas, R. Valdés, M.-C. Lafont, J. Lacaze, and B. Viguier: *Scripta Mater.*, 2006, vol. 55, pp. 191–94.
35. N. Krendelsberger, F. Weitzer, and J.C. Schuster: *Metall. Mater. Trans. A*, 2002, vol. 33A, pp. 3311–19.